Journal of Cleaner Production 235 (2019) 417–425

Contents lists available at ScienceDirect

Journal of Cleaner Production

journal homepage: www.elsevier.com/locate/jclepro

Nutrient recovery from source-diverted blackwater: Optimization for enhanced phosphorus recovery and reduced co-precipitation

Rachel A. Yee [a], Daniel S. Alessi [b], Nicholas J. Ashbolt [c], Weiduo Hao [b], Kurt Konhauser [b], Yang Liu [a, *]

[a] Department of Civil and Environmental Engineering, University of Alberta, Edmonton, T6G 2R3, Canada
[b] Department of Earth and Atmospheric Sciences, University of Alberta, Edmonton, T6G 2E3, Canada
[c] School of Public Health, University of Alberta, Edmonton, T6G 2G7, Canada

ARTICLE INFO

Article history:
Received 11 January 2019
Received in revised form
21 May 2019
Accepted 17 June 2019
Available online 20 June 2019

Handling Editor: Baoshan Huang

Keywords:
Struvite
Blackwater
Bacteria
Antimicrobial resistance genes
Metal ions

ABSTRACT

High residual phosphorus in anaerobically digested source-diverted blackwater allows for increased phosphorus recovery through struvite ($NH_4MgPO_4 \cdot 6H_2O$) precipitation. Due to the complex matrix of blackwater, recovered products inevitably contain co-precipitates of other wastewater components that have not been well characterized. The potential hazards present include pathogens, antimicrobial resistance genes (ARGs), organic and inorganic compounds. In this study, several important struvite precipitation conditions (pH, Mg^{2+}:PO_4^{3-} molar ratio and $MgCl_2$ dosing rate) were tested to determine their impact on phosphorus recovery, while taking into account the co-precipitation of enteric bacteria, ARGs and micro- and macronutrients. Results demonstrate that phosphorus recovery efficiency does not correlate to the degree of metal/microbial co-precipitation. Both PO_4^{3-} recovery and co-precipitates were affected by the operation conditions examined, and the optimal condition for nutrient recovery from blackwater was at pH 9, a 1.5:1 Mg^{2+}:PO_4^{3-} molar ratio, and a dosing rate of 24 mM min^{-1}. Although previous struvite recovery studies have identified optimal conditions for phosphorus recovery, limited information is available on the process optimization to minimize the potential risks. Downstream application of recovered struvite inevitably contains co-precipitated hazards that if not assessed can result in undesirable public health outcomes. It is necessary to evaluate struvite application and public health exposure to identify key steps that reduce public health impacts. Hence examination of struvite precipitation parameters on enhanced phosphorus recovery, along with co-precipitates, is necessary when considering the public health risk associated with efficiently recovering residual nutrients.

1. Introduction

Wastewater treatment plants (WWTPs) are often faced with scaling deposits of struvite ($NH_4MgPO_4 \cdot 6H_2O$) that can reduce treatment efficiency. Early methods applied to control struvite scaling included chemical addition of alum and ferric chloride for phosphorus removal (Mamais et al., 1994) and changes to pipe materials (Parsons and Doyle, 2002). However, with the need for new phosphorus sources to maintain agricultural practices, an increased number of investigations have directed the focus to wastewater phosphorus recovery instead of control and elimination. Struvite can be recovered and applied as a slow release fertilizer (Le Corre et al., 2009), which utilizes existing scaling deposits, reduces phosphorus release into receiving environments, and provides a source of phosphorous to maintain current agricultural practices.

Successful struvite precipitation from several types of wastewater streams have been demonstrated, where many factors, including pH, the presence of magnesium (Mg^{2+}) cations, temperature and mixing have been identified for optimized struvite precipitation (Le Corre et al., 2007; Li et al., 2012; Wang et al., 2005). Supplementing the process with Mg^{2+} has been defined as a requirement for all waste streams (Alp et al., 2008). Although there is a general consensus on the conditions that most effectively promote precipitation, consideration of the water chemistry of the specific feed source and practical issues must also be taken

* Corresponding author. 116 St & 85 Ave, Edmonton, AB, T6G 2R3, Canada.
E-mail addresses: rayee@ualberta.ca (R.A. Yee), alessi@ualberta.ca (D.S. Alessi), ashbolt@ualberta.ca (N.J. Ashbolt), whao@ualberta.ca (W. Hao), kurtk@ualberta.ca (K. Konhauser), yang.liu@ualberta.ca (Y. Liu).

https://doi.org/10.1016/j.jclepro.2019.06.191
0959-6526/

into account for any particular system. With water scarcity a worldwide concern, there is an increasing need to develop more sustainable management strategies and source-diverted blackwater (toilet water, with or without kitchen sink wastewater) has been suggested as an alternative to centralized wastewater treatment. Without the addition of other waste streams, such as greywater (shower and laundry water) and municipal wastewater (centralized wastewater collection), the carbon and nutrients available is concentrated, thus increasing ability to recover energy and nutrients (Alp et al., 2008; de Graaff et al., 2011; Gao et al., 2019). Anaerobic treatment of blackwater is effective in terms of energy recovery, but the high residual concentration of nutrients (phosphorus and nitrogen) remaining in the effluent needs to be managed (de Graaff et al., 2011; Gao et al., 2019). It is in this regard that struvite precipitation might be a suitable recovery process. Literature focusing on source-diverted blackwater is limited with respect to struvite recovery conditions. One of the few reported studies of struvite recovery from raw blackwater demonstrated that the highest phosphorus removal occurred at pH 9.5 and a 1.3:1 Mg^{2+}:PO_4^{3-} molar ratio (Alp et al., 2008). However, no study has been reported on the process optimization of anaerobically treated blackwater phosphorus recovery through struvite precipitation.

In addition to process optimization, there are several caveats that need to be further examined to identify the risks that could be involved in the use of recovered struvite. Hazards such as heavy metals, pharmaceuticals and pathogens are present in blackwater (Gell et al., 2011) and more concentrated in source-diverted streams (Gao et al., 2019); thus products derived for reuse could pose a public health concern. Evaluation of chemical and microbial co-precipitates in commercial struvite samples from wastewater indicates that co-precipitation and aggregation are likely to occur (Yee et al., 2019), however, no study has specifically linked the operational conditions with co-precipitation processes. Other studies demonstrated metal co-precipitation (e.g., K, Ca, S, Na and Fe) in struvite due to ion competition (Gell et al., 2011; Yee et al., 2019). Furthermore, calcium phosphate and carbonate co-precipitates have been identified, as Ca^{2+} is a known competitor of Mg^{2+} in struvite formation (Le Corre et al., 2005). Low levels of trace elements and nutrients could be beneficial from an agricultural perspective, thus adding value to the final product. The recovery of struvite in the form of potassium struvite ($MgKPO_4 \bullet H_2O$) could also be an attractive co-precipitate, as K^+ serves as an important macronutrient in agriculture (Mayer et al., 2016). On the other hand, trace heavy metal co-precipitation exceeding environmental standards could be problematic as plant toxicity could be induced (Nagajyoti et al., 2010).

As for the microbial risks associated with struvite co-precipitation, antimicrobial resistance (AMR) and their associated antimicrobial resistance genes (ARGs) should be considered because of their rising public health concern (WHO, 2016). While faecal indicator organisms, such as *Escherichia coli* and *Enterococcus* spp., are current regulatory indicators for wastewater effluents, spore-forming bacteria, such as *Clostridium perfringens,* could be a better indicator of persistent enteric viral and protozoan pathogens due to the increased resistance of their spores to disinfection treatment processes (De Sanctis et al., 2017). Furthermore, the threat of AMR on public health from wastewater sources and the potential genes that could be detected and persistent through treatment are not clearly defined, despite knowledge that WWTPs act as AMR reservoirs (Guo et al., 2017). A recent study examining the application of struvite on the soil profile showed that there was an increase in ARG presence following struvite application (Chen et al., 2017), which underlines the need to evaluate the co-precipitation that occurs during the formation process. However, previous studies evaluating struvite recovery from wastewater have not addressed the potential pathogen or ARG levels associated with the precipitation process.

With anaerobically digested blackwater as the source of struvite recovery due to its effectiveness for energy recovery, it is critical that potential hazards are considered in the precipitation process as a first step to considering controls for the final struvite product. Hence, the goal of this study was to identify optimal conditions for enhanced phosphorus recovery from anaerobically treated blackwater with hazard co-precipitation as an additional factor to the conventional chemical factors previously studied. Here results are presented on the effects of varying conditions (pH, Mg^{2+}:PO_4^{3-} molar ratio and $MgCl_2$ dosing rate) on struvite precipitation and co-associated metals, enteric bacteria and related ARGs within recovered struvite precipitates. Overall, this study shows the need to quantify the hazard risk involved at various steps downstream of wastewater treatment when nutrient recovery is considered.

2. Experimental

2.1. Struvite precipitation experiments

To establish a controllable system for struvite precipitation, synthetic wastewater that mimics anaerobically digested blackwater was used as the feed for all batch experiments (Table S1). Struvite precipitation experiments were conducted using a standard coagulant jar test apparatus (ESICO International, India) and titration instrument (Metrohm, Switzerland) within 1-L beakers. In each beaker, 600 mL of synthetic digested blackwater was seeded with 100 mg of lab produced struvite (in supporting information). To evaluate the co-precipitation of enteric bacterial indicators potentially reflective of the behaviour of AMR bacterial pathogens, test reactors were also spiked with *E. coli* and *C. perfringens* wastewater isolates and *E. faecalis* ATCC 51299, which carried specific gene markers (*uidA*, *entero1, cpn60, tetA, vanB & intI1*; Table S2). Pure cultures of the bacterial isolates described in Table S2 were grown overnight in trypticase soy broth (Thermo Scientific, USA) at 37 °C and washed three times with 1x PBS. Following washing, the colony forming unit (CFU) count was determined by culturing on trypticase soy agar (TSA) (Thermo Scientific, USA) and each isolate was spiked into the synthetic digested blackwater to a total concentration of approximately 10^4 cells·mL^{-1}.

To facilitate struvite precipitation, flash mixing at 200 rpm occurred for 15 min, followed by slow mixing at 100 rpm for 45 min. Following the mixing stage, the contents of the jars were allowed to settle for a minimum of 30 min in the beaker in which the experiment was conducted. The synthetic digested blackwater was centrifuged in sterile tubes at 5000 rpm for struvite collection. Overnight drying of the precipitate only occurred for the chemical analysis, while immediate DNA extractions of the wet struvite product occurred for qPCR and viability analysis, as described below.

To examine the impact of reactor operation conditions on phosphorus recovery and co-precipitation, the parameters tested included reaction pH (7, 9 and 11), Mg^{2+}:PO_4^{3-} molar ratio (1:1, 1.5:1 and 2:1, and the $MgCl_2$ dosing rate (0.1, 1, 10 and 24 mM min^{-1}). Sterile 1 M NaOH was used to adjust the pH to the appropriate level. The addition of Mg^{2+} required to meet the Mg^{2+}:PO_4^{3-} molar ratio was calculated based on the addition of sterile 1 M $MgCl_2$ and all chemicals were added during the flash mixing stage. $MgCl_2$ dosing rates were controlled by using the Tiamo (Metrohm, Switzerland) software that was used in conjunction with the titrator.

2.2. Chemical analysis

Phosphorus kits (TNT844, Hach, USA) were used to measure PO_4^{3-}-P concentrations before and after precipitation. Several techniques were utilized at the University of Alberta to assist with characterization of the struvite samples under varying conditions. The struvite composition was analyzed via X-ray diffraction (XRD; Rigaku Ultimate IV, Japan) with copper radiation and peak comparison to the Inorganic Crystal Structure Database (ICSD) using the reference struvite cards – PDF #97-006-0626 and PDF #98-000-0419 (http://www2.fiz-karlsruhe.de/icsd_home.html). The struvite morphology was examined via scanning electron microscopy (SEM; Zeiss Sigma 300 VP-FESEM, USA) and energy dispersive X-ray spectroscopy (EDS; Bruker EDS System, USA). The struvite samples were also analyzed for metal composition and concentrations via induced coupled plasma optical emission spectrometry (ICP-OES; Thermo iCAP 6000 series, Thermo Scientific, USA). Dry samples (0.04–0.07 g) were digested in 5 mL of trace metal grade nitric acid (Thermo Fisher Scientific, USA) following Method 3051A as set by the U.S. EPA (US. EPA, 2007). Digested samples were diluted to a volume of 25 mL with distilled water prior to ICP-OES analysis in triplicate.

2.3. qPCR analysis

DNA extractions were undertaken on wet struvite samples (0.15–0.2 g w/w) with the PowerSoil DNA extraction kit™ (Qiagen, Germany) as per the manufacturer's protocol. DNA extractions were conducted on 500 μL supernatant samples by placing tubes on a heat block at 95 °C for 15 min. Primer and probe sets for all genes of interest were previously developed and described in Table S2. An internal amplification control (Deer et al., 2010), also listed in Table S2, was used with the *uidA* assay to ensure that inhibition of the samples was not occurring during the qPCR reaction. Cycling conditions and reaction specifics have been previously described (Yee et al., 2019).

2.4. Viability analysis

Colilert and Enterolert (IDEXX, USA) were utilized to estimate culturable spiked *E. coli* and *E. faecalis* cells in recovered struvite as most probable numbers (MPNs) as per the manufacturer's recommendations. By contrast, *C. perfringens* spores were estimated as CFUs using CM0587 Perfringens agar base (TSC & SFP) media (Thermo Scientific, USA) with 85 mg/L 4-methylumbelliferyl phosphate (Invitrogen, USA) to identify colonies by fluorescence under UV light (Davies et al., 1995). Wet samples of struvite (0.1–0.2 g) were centrifuged and washed twice with sterile 1x PBS. The washed samples were re-suspended in 1 mL of sterile 1x PBS. Following resuspension, 1:10 serial dilutions were performed and 100 μL samples of the dilutions were used for quantification. Quanti-trays 2000™ (IDEXX, USA) were incubated overnight according to the manufacturer's protocols and agar plates at 35 °C for up to 48 h.

2.5. Zeta potential analysis

Overnight cultures of the bacterial isolates were centrifuged and washed thrice with 1x PBS and separately spiked into synthetic wastewater that was adjusted to a pH of 7, 9 or 11 with sterile 1 M NaOH. Following the pH adjustment, the zeta potential was measured in folded capillary zeta cells (Zetasizer nano series, Malvern, UK). Triplicate values were obtained and based on 20 measurements of the sample.

2.6. Microbial hydrophobicity analysis

The hydrophobicity of bacterial isolates was determined with the microbial adhesion to hydrocarbons (MATH) assay via simultaneously measuring the change in absorbance as well as by counting CFUs on a TSA plate (Qiao et al., 2012). Overnight cultures of *E. coli*, *E. faecalis* and *C. perfringens* isolates were centrifuged and washed three times with 1x PBS. The cultures were adjusted to an optical density of 1.0 measured at an absorbance of 600 nm. 300 μL of filter sterile hexadecane was added to 5 mL of cells and vortexed for 2 min. The tubes were allowed to rest for a minimum of 15 min for separation to occur and the final absorbance at 600 nm was measured. Serial dilutions were performed with the measured cells before and after hexadecane addition and 100 μL was plated on TSA plates for colony growth. The following formula was used to determine the fraction partitioned to the hydrocarbon phase (% Adh) based on the absorbance readings or CFU counts, represented as C:

$$\%\ \text{Adh} = [1\text{-}C_{\text{aqueous phase}}/C_{\text{original bacteria suspension}}] \times 100$$

% Adh corresponds to high (≥70%), moderate (50–70%) and low hydrophobicity (<50%). All tests were conducted in triplicate for each isolate.

2.7. Mineral precipitation modelling

Mineral precipitation modelling was conducted in the absence of organics to qualitatively assess the minerals that could potentially precipitate. The modelling process was conducted with PHREEQC 3.4.0 using K_{sp} values of minerals from the database of MINTEQ version 4. The ion activity products (IAP) of potential precipitated minerals are calculated and compared with their solubility constants (K_{sp} values) to predict the possibility of mineral precipitation. The saturation index (SI) values were used to determine the potential for certain compounds to co-precipitate at the tested conditions.

$$\text{SI} = \log_{10}(\text{IAP}/K_{sp})$$

To be specific, two solutions were simulated in the modelling procedure: one is synthetic blackwater and the other is 1M $MgCl_2$ solution. Once the individual solutions were simulated, mixing models were performed based on the mixture of the two solutions with various Mg^{2+}:PO_4^{3-} molar ratios. A gas phase consisting CO_2 (partial pressure $10^{-3.5}$) was also included in simulating procedure to mimic the solution in equilibrium with atmospheric CO_2.

3. Results and discussion

3.1. Morphological analysis

Similar XRD peak positions as determined by Bragg's law were observed for all samples tested (Figure S1) and crystalline struvite was confirmed under all conditions examined by comparison with the Inorganic Crystal Structure Database (Jian and Hejing, 2003). Minor differences in observed peak heights (Figure S1) are probably due to the organization of the sample on the mount during the analysis process (Jian and Hejing, 2003). The low level of background noise indicates that the samples are crystalline, with co-precipitates that cannot be determined with this analysis method due to their amorphous nature.

An initial determination of the physical characteristics of the co-precipitates associated with struvite formed under different water chemistries was provided by SEM-EDS analyses. All samples

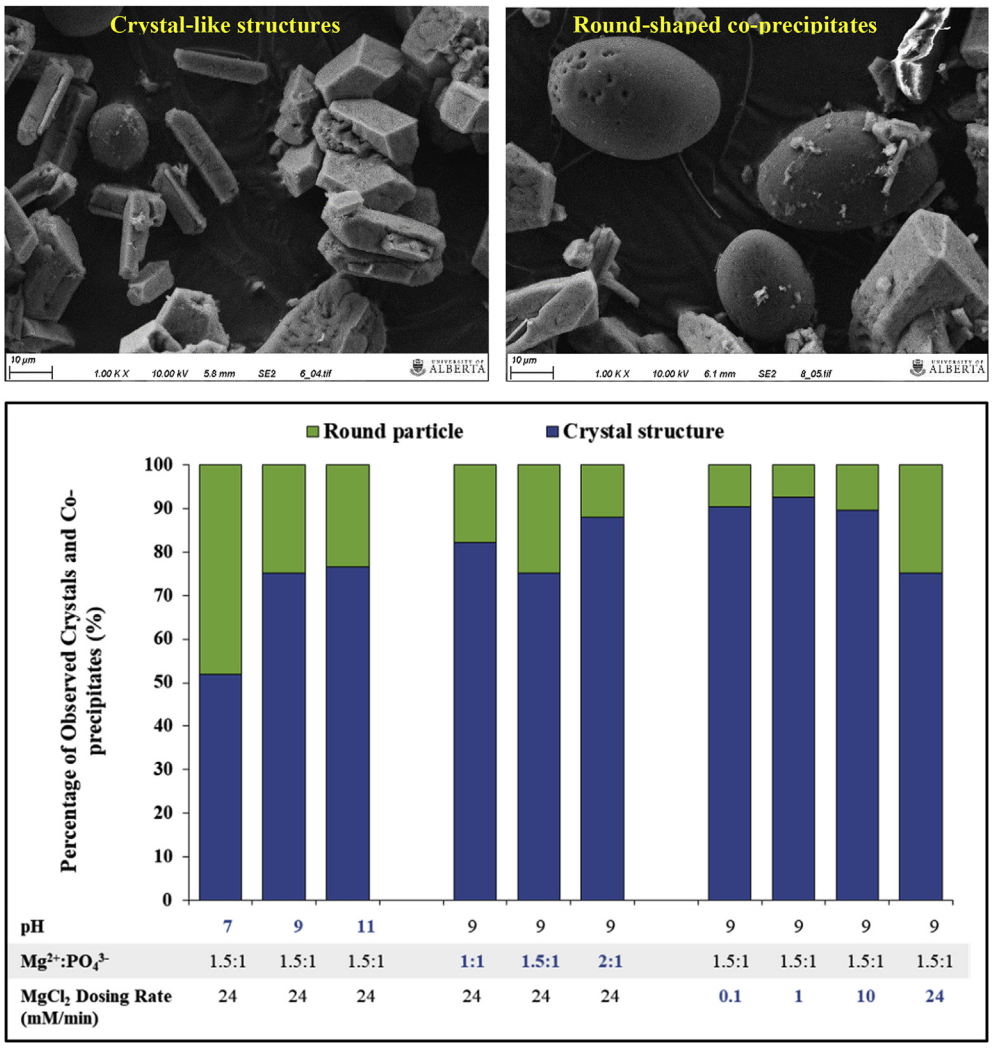

Fig. 1. Qualitative analysis of crystal structures and round co-precipitates observed. Top images represent SEM images (1000x magnification) of crystal structures (left) and round particles (right). Bottom graph represents estimated percentage of crystals and round particles in images (N = 9 fields of view).

appeared to contain two different morphologies – elongated and round-shaped structures (Fig. 1). Following a 60 min reaction time, elongated crystalline structures (20–40 μm), some with growth in multiple directions, appeared; representing the development of struvite precipitates. At lower $MgCl_2$ dosing rates (10 mM min^{-1} and under) crystals were more rectangular shaped and elongated as shown in Fig. 1. At a dosing rate of 24 mM min^{-1}, growth occurred in multiple directions making it difficult to morphologically define. Differences in morphology have been previously attributed to chemical conditions, such as temperature, ion concentration and pH, which impact the interactions between ions (Tansel et al., 2018). With concentrated waste streams, increased impurity concentrations can result in changes in growth patterns (Tansel et al., 2018). As a result, struvite has been described in various forms including needle-shaped, star-shaped, X-shaped and pyramidal (Tansel et al., 2018). Surface chemical analysis of the round-shaped compounds, which present a non-crystal-like shape, appear to be organic molecules with traces of P, Mg and Ca that formed in parallel to struvite from the blackwater matrix. Estimating the relative percentage between the crystal-like compounds and amorphous co-precipitates can be made by particle counting of the SEM images. As observed in Fig. 1, the struvite crystals dominate in the images. As pH increased from 7 to 11 there was reduced observed co-precipitation, while increasing the Mg^{2+} dosing rate above 10 mM min^{-1} increased co-precipitation.

The EDS results (Figure S2-S4) further confirms the presence of struvite as might be expected with a Mg:Ca ratio of ~1:1. Based on the EDS results, it is likely the round particles are carbonate minerals, such as calcium-magnesium carbonates or calcium phosphate that simultaneously co-precipitate. It should also be noted that EDS provides an analysis of the surface composition and therefore is not representative of all potential co-precipitation.

3.2. Phosphorus recovery and Co-preciptiates

As shown in Fig. 2a, increasing the pH of the wastewater resulted in an upward trend of PO_4^{3-}-P recovery ($p < 0.05$). PO_4^{3-}-P recovery greater than 83% can be acheived under pH 9 and 11 conditions, although the recovery is not significantly improved by increasing the pH to 11. According to mineral precipitation modelling (Table S3), at a pH of 9 and 11, $CaHPO_4$ and vivianite (both PO_4^{3-} bearing minerals) precipitate, which is not observed at a pH of 7 condition. This could explain why PO_4^{3-} recovery experienced a significant increase when pH increased from 7 to 9. Meanwhile, at a pH of 11, new minerals like aragonite, $Ca_3(PO_4)_2$, $Ca_4H(PO_4)_3 \bullet 3H_2O$, $CaHPO_4 \bullet 2H_2O$, $CaCO_3$, dolomite, $Fe_3(OH)_8$, (PO_4^{3-}

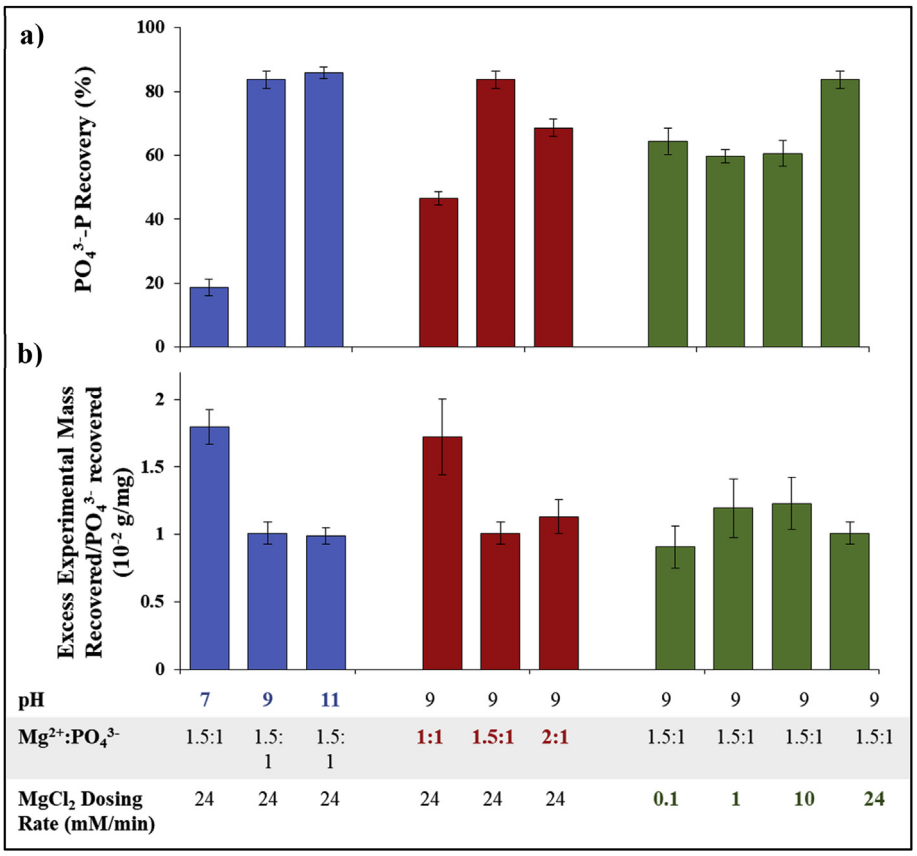

Fig. 2. PO_4^{3-}-P recovery (%) and excess experimental mass recovered per PO_4^{3-} recovered (10^{-2} g mg^{-1}) of tested conditions from blackwater (N = 3, error bars indicate standard deviation).

and non-PO_4^{3-} bearing minerals) appear to precipitate, which could partially explain why P recovery increased but not significantly when pH increased from 9 to 11. Similar results have been reported for other waste streams with struvite predominately forming when the pH is above 9 (Mehta and Batstone, 2013; Shih et al., 2017; Tang, 2016).

As Mg^{2+} ions are often limiting, the Mg^{2+}:PO_4^{3-} molar ratio can also affect recovery. In the current study, it was observed that manipulation of the Mg^{2+}:PO_4^{3-} molar ratio from 1:1 to 1.5:1 resulted in increased PO_4^{3-}- P recovery from 46% to 69% ($p < 0.05$). Further increases in Mg^{2+} to a 2:1 Mg^{2+}:PO_4^{3-} molar ratio did not improve recovery, which is consistent with previous studies that demonstrated a 1:1 M ratio is beneficial, but exceeding that did not greatly improve PO_4^{3-}-P recovery (Kim et al., 2017). Furthermore, mineral precipitation modelling did not show a difference in the minerals that could potentially co-preciptiation when the Mg^{2+}:PO_4^{3-} was altered. Lastly, $MgCl_2$ dosing rate changes did not impact PO_4^{3-}-P recovery efficiency ($p > 0.05$) until the dosing rate exceeded 10 mM min^{-1}, which appeared to improve PO_4^{3-}-P recovery, likely due to the rapid struvite formation that occurs with rapid dosing.

Further, the theortical amount of struvite in the collected samples was used as a baseline value to determine co-precipitation of other PO_4^{3-}-P salts. As shown in Fig. 2b, the trend of the excess mass collected per gram of PO_4^{3-}-P recovered differs from expected struvite PO_4^{3-}-P recovery. At pH 7, a lower percentage of PO_4^{3-}-P recovery occurred compared to higher pH conditions ($p < 0.05$), hence a large amount of the mass collected cannot be attributed to struvite. A low Mg^{2+}:PO_4^{3-} molar ratio of 1:1 presents a higher excess mass recovered per PO_4^{3-}-P removed, also with a low PO_4^{3-}-P recovery percentage. This is no surprise, as a lower availability of Mg^{2+} would allow for other cations, such as Ca^{2+}, that is a competitor ion of Mg^{2+} in the formation of phosphate precipitates (Le Corre et al., 2005). The metal analysis, as discussed below, is also consistent with the low excess mass observed when the molar ratio exceeded 1:1 ($p < 0.05$). Further, a higher dosing rate may result in increased co-precipitation as a more rapid addition of Mg^{2+} into the system may induce rapid struvite preciptiation that would entrap ions and microbes during crystal formation. On the other hand, high dosing rates can also enhance the rate of PO_4^{3-}-P recovery with no significant difference in excess mass ($p > 0.05$). Fig. 2 shows that under the highest dosing rate condition tested with a pH of 9 and a 1.5:1 Mg^{2+}:PO_4^{3-} molar ratio, high PO_4^{3-}-P recovery and relatively low co-precipitation was observed. These conditions represent the optimal conditions tested in the current study.

3.3. Metal Co-precipitation

Fig. 3 depicts the ICP-OES analysis of the major metals detected following struvite precipitation, a likely scenrio as macronutrients (Ca, Na, K and S) have been previously observed in blackwater effluents (Moges et al., 2018) In general, an increased pH and $MgCl_2$ dosing rate and a low Mg^{2+}:PO_4^{3-} molar ratio increased metal co-precipitation. Under all conditions, Ca^{2+}, Ni^{2+} and K^+ ions dominated the metals detected. The formation of potassium struvite ($MgKPO_4 \bullet 6H_2O$), though not shown in the modelling results has also been linked with increased pH levels. In the current study, it was experimentally observed at or above pH 9 or at higher

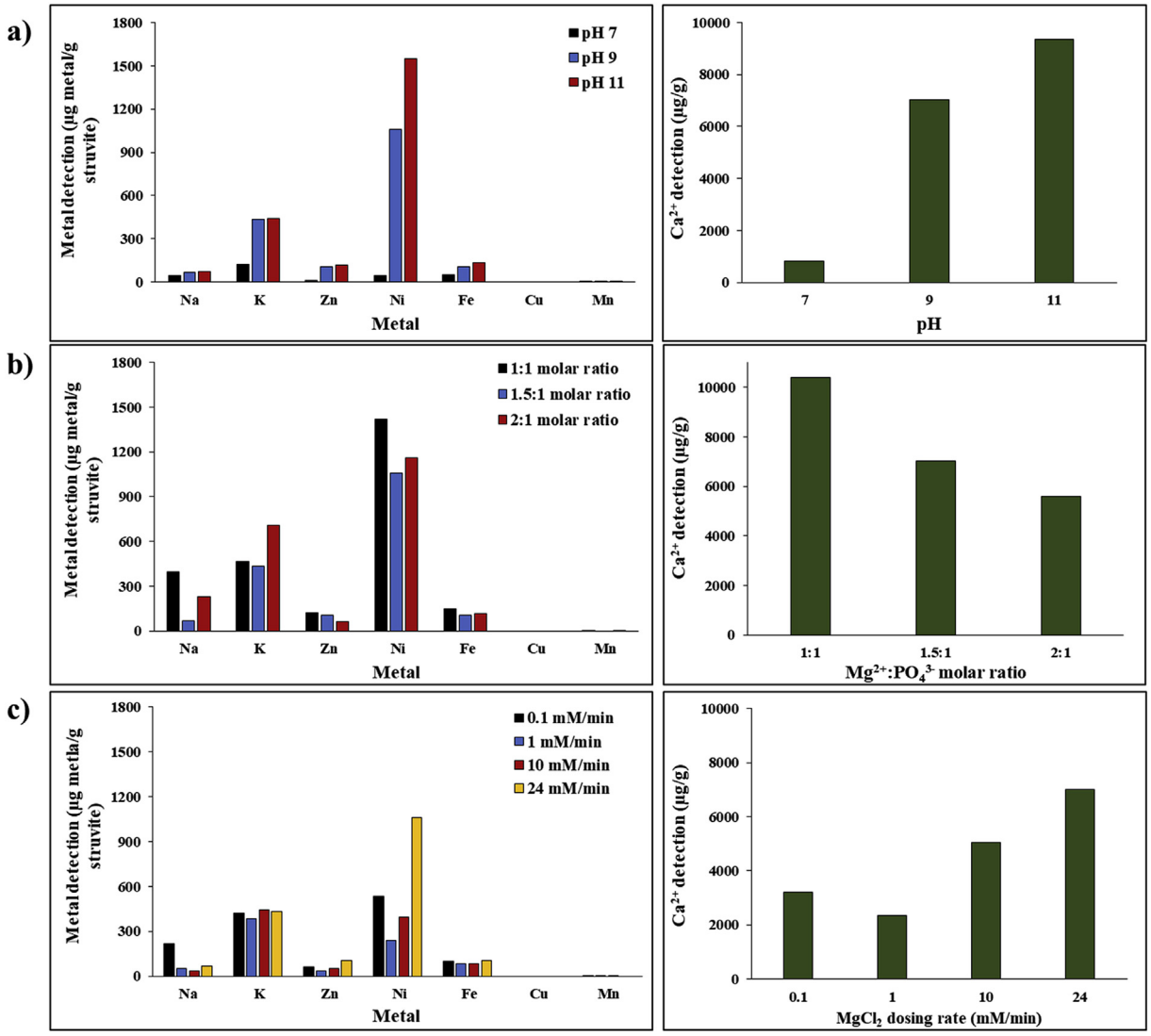

Fig. 3. ICP-OES analysis of dominant metals in struvite samples produced from blackwater (N = 3; standard deviation not shown). a) pH 7, 9 and 11; b) 1:1, 1.5:1 and 2:1 Mg^{2+}:PO_4^{3-} molar ratio; c) 0.1 mM min^{-1}, 1 mM min^{-1}, 10 mM min^{-1} and 24 mM min^{-1} $MgCl_2$ dosing rate.

Mg^{2+}:PO_4^{3-} molar ratios. As supersaturation helps dictate precipitation and $MgKPO_4 \bullet 6H_2O$ is less soluble than $MgNH_4PO_4 \bullet 6H_2O$, the increased Mg^{2+} would also drive the reaction to favour potassium struvite (Bennett et al., 2017). Additionally, higher detection of Ca^{2+} and Ni^{2+} was observed when there was less Mg^{2+} in the system as those cations can replace Mg^{2+} in the formation process. Based on the greater calculated mass at a pH of 7, it would be expected that metals and organics would account for the observation precipitation. However, the inconsistency in comparison with the ICP-OES analysis and modelling shows that experimentally, other PO_4^{3-} compounds interfere with the co-precipitation calculations above, which could be attributed to the organic ligand that existed in blackwater (Le Corre et al., 2005). Several calcium phosphate and carbonate compounds were theoretically determined to precipitate at a higher pH in the model, however, other phosphate compounds would not affect the calculated PO_4^{3-} recovery as described in Fig. 1, as a 1:1:1 M ratio is still required. As a result, it is likely that pure struvite was not recovered, though, the recovery of other phosphate compounds can be more useful from an agricultural point of view with the role of bacteria in recovery discussed next.

3.4. Bacterial viability and gene detection

Culture tests and qPCR analysis on recovered struvite samples show that detection of bacterial genes and ARG targets occurs in all samples, though pH appeared to have an effect on the viability of *E. coli* cells (Fig. 4). At a pH of 11, the viability of spiked *E. coli* cells decreased, while the *E. faecalis* and *C. perfringens* cell viability remained unchanged across all pH conditions tested, an expected observation given the knowledge they are more resistant to changing environments (Korajkic et al., 2014). Though it may be predicted that a pH of 9 would also reduce *E. coli* viability (Parhad and Rao, 1974), the results indicated the resilence of environmental isolates over culture collection lab strains. Of the molar ratio and dosing rate conditions tested, the fraction of viable cells did not differ ($p > 0.05$), indicating that Mg^{2+} concentration and rate of $MgCl_2$ addition appear to play a larger role in metal co-precipitation than on cell viability (Fig. 4). Utilizing qPCR to determine the percentage of spiked quantified genes that partition from the liquid to solid phase did not appear to result in an obvious gene precipitation trend nor could gene expression be confirmed. The similar percentages observed between the genes that identify specific bacteria

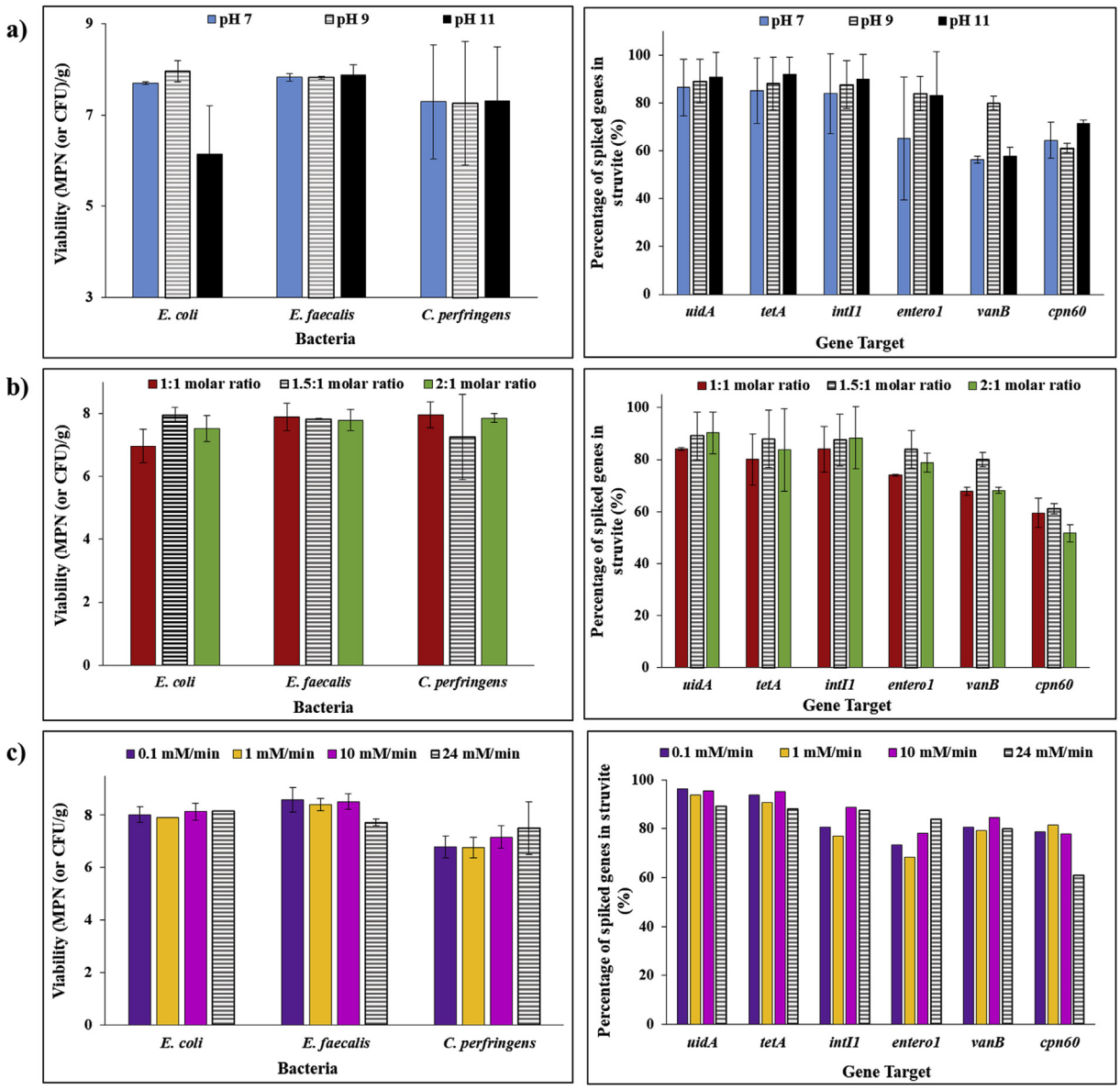

Fig. 4. Viable cell estimates (left) and percent qPCR positive (right) from struvite produced at varying tested conditions. a) pH 7, 9 and 11; b) 1:1, 1.5:1 and 2:1 Mg^{2+}:PO_4^{3-} molar ratio; c) 0.1 mM min^{-1}, 1 mM min^{-1}, 10 mM min^{-1} and 24 mM min^{-1} $MgCl_2$ dosing rate. (N = 2 for all results except for gene analysis of dosing rate (N = 1); error bars represent standard deviation).

and their associated ARGs supports co-precipitation of spiked strains rather than external contamination effects. Furthermore, the ARG targets were selected based on their likely presence in wastewater, and though the detection of these targets in struvite cannot be used to directly predict the potential spread of AMR through horizontal gene transfer, it is important to consider that co-associated microbes within recovered struvite could be a risk that requires further evaluation (Chen et al., 2017). Chen and colleagues (Chen et al., 2017) have previously shown that the ARGs within applied struvite can also end up in soil bacteria and on harvested crops, further supporting the need to evaluate this risk.

Despite the lack of trend associated with microbial detection, characterization of the cell surface through zeta potential and hydrophobicity measurements can also provide insights into the role of microbes in mineral co-preciptiation. The surface charge of *C. perfringens* exposed to wastewater was represented by a positive zeta potential (0–3 mV) that indicates the increased likelihood of cell aggregation within the system. Hydrophobicity results show that there was indeed a difference in the percent of cells that adhere to hexadecane following addition (Table S4). In these assays, *C. perfringens* resulted in a more hydrophilic surface than the vegetative cells of the *E. coli* and *E. faecalis* isolates used (Wiencek et al., 1990). The hydrophilic nature of *C. perfringens* and the ability of its cells to aggregate could indicate that they would be more likely to interact with molecules during the precipitation process. Further studies into the effect of microbe surface properties would help further explain their co-precipitation with struvite. Additionally, the inactivation and removal of pathogens will require evaluation to further reduce the risk. Initial studies on recovered fertilizer from source-separated urine has shown that washing and drying methods can assist in pathogen inactivation and removal to improve struvite quality (Bischel et al., 2015). Increased drying temperatures increased bacteria inactivation and drying and storage can impact re-growth as moisture content plays a large role

(Bischel et al., 2016). Therefore, post precipitation treatment processes, such as drying will be essential to mitigate the risk involved with nutrient recovery from blackwater.

3.5. Conclusion

Given the results presented, it is clear that a degree of metal and microbe co-precipitation is likely to occur when recovering phosphate and ammonium nutrients by struvite precipitation. The degree of co-precipitation does not correlate to the phosphorus recovery efficiency, and is highly dependent on the nature of the feed and precipitation conditions, as interactions between matrix ions and microbes will dictate the precipitation process. The modelling results further support the variability of co-precipitation that can occur when conditions are altered and indicates that pH plays a large role in the mineral co-precipitation that can occur. In summary, the optimal conditions demonstrated for enhanced PO_4^{3-}-P recovery with minimized co-precipitation from blackwater are a pH of 9, a 1.5:1 Mg^{2+}:PO_4^{3-} molar ratio, and a 24 mL min^{-1} $MgCl_2$ dosing rate. Metal co-precipitation occurred under all conditions and the presence of some micro- and macro-nutrients could be beneficial if the resulting struvite is used for agriculture. Ultimately, the study shows that a health risk does exist in the process of struvite recovery from blackwater. As the co-precipitation of hazards differ at varying parameters, the potential risk associated with reuse would also differ. Production and collection process optimization can assist in mitigating risk; however, optimization of post precipitation options have yet to be examined to reduce the microbial issues that exist, though could include struvite heat-drying.

Declarations of interest

None.

Acknowledgements

The work was financially supported by Natural Sciences and Engineering Research Council (NSERC) — Collaborative Research and Development (CRD) project and Industrial Research Chair (IRC) program, EPCOR Water Services, EPCOR Drainage Services, Alberta Innovates and WaterWerx. Dr. Liu acknowledges the Canada Research Chair (CRC) program. The authors thank Candis Scott and Nancy Price (School of Public Health, University of Alberta) for molecular/microbiological training and technical support as well as Johnathon Shim (Department of Civil and Environmental Engineering, University of Alberta) for lab assistance.

Appendix A. Supplementary data

Supplementary data to this article can be found online at https://doi.org/10.1016/j.jclepro.2019.06.191.

References

Alp, Ö., Yazgan, B., Söhmen, U., Gulyas, H., Otterpohl, R., 2008. Recovery of Phosphorus as Struvite from Source-Separated Blackwater.

Bennett, A.M., Lobanov, S., Koch, F.A., Mavinic, D.S., 2017. Improving potassium recovery with new solubility product values for K-struvite. J. Environ. Eng. Sci. 12, 93–103. https://doi.org/10.1680/jenes.17.00019.

Bischel, H.N., Özel Duygan, B.D., Strande, L., McArdell, C.S., Udert, K.M., Kohn, T., 2015. Pathogens and pharmaceuticals in source-separated urine in eThekwini, South Africa. Water Res. 85, 57–65. https://doi.org/10.1016/j.watres.2015.08.022.

Bischel, H.N., Schindelholz, S., Schoger, M., Decrey, L., Buckley, C.A., Udert, K.M., Kohn, T., 2016. Bacteria inactivation during the drying of struvite fertilizers produced from stored urine. Environ. Sci. Technol. 50, 13013–13023. https://doi.org/10.1021/acs.est.6b03555.

Chen, Q., An, X., Zhu, Y., Su, J., Gillings, M.R., Ye, Z., 2017. Application of struvite alters the antibiotic resistome in soil, rhizosphere, and phyllosphere. Environ. Sci. Technol. 51, 8149–8157. https://doi.org/10.1021/acs.est.7b01420.

Davies, C.M., Long, J.A.H., Donald, M., Ashbolt, N.J., 1995. Survival of fecal microorganisms in marine and freshwater sediments. Appl. Environ. Microbiol. 61, 1888–1896.

de Graaff, M.S., Temmink, H., Zeeman, G., Buisman, C.J.N., 2011. Energy and phosphorus recovery from black water. Water Sci. Technol. 63, 2759–2765. https://doi.org/10.2166/wst.2011.558.

De Sanctis, M., Del Moro, G., Chimienti, S., Ritelli, P., Levantesi, C., Di Iaconi, C., 2017. Removal of pollutants and pathogens by a simplified treatment scheme for municipal wastewater reuse in agriculture. Sci. Total Environ. 580, 17–25. https://doi.org/10.1016/j.scitotenv.2016.12.002.

Deer, D.M., Lampel, K.A., González-Escalona, N., 2010. A versatile internal control for use as DNA in real-time PCR and as RNA in real-time reverse transcription PCR assays. Lett. Appl. Microbiol. 50, 366–372. https://doi.org/10.1111/j.1472-765X.2010.02804.x.

Gao, M., Zhang, L., Florentino, A.P., Liu, Y., 2019. Performance of anaerobic treatment of blackwater collected from different toilet flushing systems : can we achieve both energy recovery and water conservation? J. Hazard Mater. 365, 44–52. https://doi.org/10.1016/j.jhazmat.2018.10.055.

Gell, K., Ruijter, F.J. d., Kuntke, P., Graaff, M., De Smit, A.L., 2011. Safety and effectiveness of struvite from black water and urine as a phosphorus fertilizer. J. Agric. Sci. 3, 67–80. https://doi.org/10.5539/jas.v3n3p67.

Guo, J., Li, J., Chen, H., Bond, P.L., Yuan, Z., 2017. Metagenomic analysis reveals wastewater treatment plants as hotspots of antibiotic resistance genes and mobile genetic elements. Water Res. 123, 468–478. https://doi.org/10.1016/j.watres.2017.07.002.

Jian, Z., Hejing, W., 2003. The physical meanings of 5 basic parameters for an x-ray diffraction peak and their application. Chin. J. Geochem. 22, 38–44.

Kim, D., Min, K.J., Lee, K., Yu, M.S., Park, K.Y., 2017. Effects of pH, molar ratios and pre-treatment on phosphorus recovery through struvite crystallization from effluent of anaerobically digested swine wastewater. Environ. Eng. Res. 22, 12–18. https://doi.org/10.4491/eer.2016.037.

Korajkic, A., McMinn, B.R., Shanks, O.C., Sivaganesan, M., Fout, G.S., Ashbolt, N.J., 2014. Biotic interactions and sunlight affect persistence of fecal indicator bacteria and microbial source tracking genetic markers in the upper Mississippi river. Appl. Environ. Microbiol. 80, 3952–3961. https://doi.org/10.1128/AEM.00388-14.

Le Corre, K.S., Valsami-jones, E., Hobbs, P., Parsons, S.A., 2005. Impact of calcium on struvite crystal size, shape and purity. J. Cryst. Growth 283, 514–522. https://doi.org/10.1016/j.jcrysgro.2005.06.012.

Le Corre, K.S., Valsami-Jones, E., Hobbs, P., Parsons, S.A., 2009. Phosphorus recovery from wastewater by struvite crystallization: a review. Crit. Rev. Environ. Sci. Technol. 39, 433–477. https://doi.org/10.1080/10643380701640573.

Le Corre, K.S., Valsami-Jones, E., Hobbs, P., Parsons, S.A., 2007. Impact of reactor operation on success of struvite precipitation from synthetic liquors. Environ. Technol. 28, 1245–1256. https://doi.org/10.1080/09593332808618885.

Li, Z., Ren, X., Zuo, J., Liu, Y., Duan, E., Yang, J., Chen, P., Wang, Y., 2012. Struvite precipitation for ammonia nitrogen removal in 7-aminocephalosporanic acid wastewater. Molecules 17, 2126–2139. https://doi.org/10.3390/molecules17022126.

Mamais, D., Pitt, P.A., Cheng, Y.W., Loiacono, J., Jenkins, D., Wen, Y., 1994. Digesters determination to control in anaerobic of ferric chloride precipitation digesters dose struvite sludge. Water Environ. Res. 66, 912–918.

Mayer, B.K., Baker, L.A., Boyer, T.H., Drechsel, P., Gifford, M., Hanjra, M.A., Parameswaran, P., Stoltzfus, J., Westerhoff, P., Rittmann, B.E., 2016. Total value of phosphorus recovery. Environ. Sci. Technol. 50, 6606–6620. https://doi.org/10.1021/acs.est.6b01239.

Mehta, C.M., Batstone, D.J., 2013. Nucleation and growth kinetics of struvite crystallization. Water Res. 47, 2890–2900. https://doi.org/10.1016/j.watres.2013.03.007.

Moges, M.E., Todt, D., Heistad, A., 2018. Treatment of source-separated blackwater : a decentralized strategy for nutrient recovery towards a circular economy. Water 10, 1–15. https://doi.org/10.3390/w10040463.

Nagajyoti, P.C., Lee, K.D., Sreekanth, T.V.M., 2010. Heavy metals, occurrence and toxicity for plants: a review. Environ. Chem. Lett. 8, 199–216. https://doi.org/10.1007/s10311-010-0297-8.

Parhad, N.M., Rao, N.U., 1974. Effect of pH on survival of *Escherichia coli*. Water Environ. Fed. 46, 980–986.

Parsons, S.A., Doyle, J.D., 2002. Struvite scale formation and control. Water Sci. Technol. 49, 177–182.

Qiao, G., Li, H., Xu, D.-H., Il Park, S., 2012. Modified a colony forming unit microbial adherence to hydrocarbons assay and evaluated cell surface hydrophobicity and biofilm production of *Vibrio scophthalmi*. J. Bacteriol. Parasitol. 3, 1–6. https://doi.org/10.4172/2155-9597.1000130.

Shih, Y.-J., Abarca, R.R.M., de Luna, M.D.G., Huang, Y.-H., Lu, M.-C., 2017. Recovery of phosphorus from synthetic wastewaters by struvite crystallization in a fluidized-bed reactor: effects of pH, phosphate concentration and coexisting ions. Chemosphere 173, 466–473. https://doi.org/10.1016/j.chemosphere.2017.01.088.

Tang, P., 2016. Effects of solution pH and seed material on MAP crystallization. Int. J. Environ. Prot. Policy 4, 171–177. https://doi.org/10.11648/j.ijepp.20160406.13.

Tansel, B., Lunn, G., Monje, O., 2018. Struvite formation and decomposition characteristics for ammonia and phosphorus recovery: a review of magnesium-ammonia-phosphate interactions. Chemosphere 194, 504–514. https://

doi.org/10.1016/j.chemosphere.2017.12.004.
US. EPA, 2007. Method 3051A - Microwave Assisted Acid Digestion of Sediments, Sludges, Soils and Oils.
Wang, J., Burken, J.G., Zhang, X., Surampalli, R., 2005. Engineered struvite precipitation: impacts of component-ion molar ratios and pH. J. Environ. Eng. 131, 1433–1440. https://doi.org/10.1061/(ASCE)0733-9372 (2005)131:10(1433).
WHO, 2016. Global Priority List of Antibiotic-Resistant Bacteria to Guide Research, Discovery, and Development of New Antibiotics. https://doi.org/10.1016/S1473-3099(09)70222-1.
Wiencek, K.M., Klapes, N.A., Foegeding, P.M., 1990. Hydrophobicity of Bacillus and Clostridium spores. Appl. Environ. Microbiol. 56, 2600–2605, 0099-2240/90/092600-06.
Yee, R.A., Leifels, M., Scott, C., Ashbolt, N.J., Liu, Y., 2019. Evaluating microbial and chemical hazards in commercial struvite recovered from wastewater. Environ. Sci. Technol. 53, 5378–5386. https://doi.org/10.1021/acs.est.8b03683.